



<b>Title</b>	<b>Multiple cations interdiffusion in <math>\text{In}_{0.53}\text{Ga}_{0.47}\text{As}/\text{In}_{0.52}\text{Al}_{0.48}\text{As}</math> quantum well</b>
<b>Author(s)</b>	<b>Chan, Y; Shiu, WC; Tsui, WK; Li, EH</b>
<b>Citation</b>	<b>Materials Research Society Symposium Proceedings, Boston, MA., 2-5 December 1996, v. 450, p. 377-382</b>
<b>Issued Date</b>	<b>1997</b>
<b>URL</b>	<b><a href="http://hdl.handle.net/10722/46022">http://hdl.handle.net/10722/46022</a></b>
<b>Rights</b>	<b>Materials Research Society Symposium Proceedings. Copyright © Materials Research Society.</b>

# Multiple Cations Interdiffusion in $\text{In}_{0.53}\text{Ga}_{0.47}\text{As}/\text{In}_{0.52}\text{Al}_{0.48}\text{As}$ Quantum Well

Y. Chan\* , W.C. Shiu\*\* , W.K. Tsui\* , and E. Herbert Li\*

\* University of Hong Kong, Department of Electrical and Electronic Engineering, Pokfulam Road, Hong Kong.

\*\*Hong Kong Baptist University, Department of Mathematics, Kowloon, Hong Kong.

## Abstract

Multiple cations interdiffusion in  $\text{In}_{0.53}\text{Ga}_{0.47}\text{As}/\text{In}_{0.52}\text{Al}_{0.48}\text{As}$  quantum well (QW) structure is investigated by using the model of expanded form of Fick's second law. The model is fitted to the measured concentration data in order to determine their diffusion coefficients. Once the concentration distribution is obtained, the types of strain and their variation across the QW can be determined, thus the subbands and transitions can be gathered. Result shows interesting phenomena due to this three species interdiffusion.

## 1. Introduction

There are immense interests in the InGaAs/InAlAs QW which are lattice matched to InP substrate. This is because of their application in the fabrication of optoelectronic devices operating in the 1.3 -1.6  $\mu\text{m}$  spectral range, as well as for high field devices. Recently InGaAs/InAlAs heterostructures have been grown by molecular beam epitaxy (MBE) on InP substrates in single and multiple quantum wells[1]. This new material system have so far been concentrated on the transport properties of high mobility two-dimensional electron gas at single interfaces[2], the achievement of laser action[3], and the variation of luminescence energy as a function of quantum well thickness[4]. The application of thermal processing of QW materials is now extended to both multiple species and phases. Recent reports have been put effort towards two species interdiffusion considering only one effective diffusion coefficient[5,6]. Although, after diffusion, this system only confines to the III metals but it consists of three interdiffused elements. This complicates the diffusion process because it cannot be described by the simple one diffusion coefficient model. To understand the interdiffusion mechanism in this multiple species, all the three diffused elements (Al, In, Ga) should be described by their own diffusion rate together with the cross rates.

## 2. Modeling

### A. Effects of disordering

A number of models have been presented for investigating interdiffusion involving the use of only one error function in approximating the compositional profiles.  $\text{In}_{0.53}\text{Ga}_{0.47}\text{As}/\text{In}_{0.52}\text{Al}_{0.48}\text{As}$  Diffused QW (DFQW) can be complicated by the fact that the interdiffusion of the group III metals cannot necessarily be described by a single effective diffusion coefficients. In order to give a comprehensive DFQW of this model, we have modeled the above system by the expanded form of Fick's second law:

$$\frac{\partial C_1}{\partial t} = \frac{\partial}{\partial z} \left( D_{11} \frac{\partial C_1}{\partial z} \right) + \frac{\partial}{\partial z} \left( D_{12} \frac{\partial C_2}{\partial z} \right) \quad (1)$$

$$\frac{\partial C_2}{\partial t} = \frac{\partial}{\partial z} \left( D_{21} \frac{\partial C_1}{\partial z} \right) + \frac{\partial}{\partial z} \left( D_{22} \frac{\partial C_2}{\partial z} \right) \quad (2)$$

where  $t$  is time,  $C_1$  and  $C_2$  are concentrations of In and Ga respectively,  $t$  is time,  $D_{ij}$  ( $i,j=1,2$ ) are the diffusion coefficients,  $D_{ii}$  is the diffusion rate of species  $i$  and  $D_{ij}$  is the cross diffusion rate between species  $i$  and  $j$ ,  $z$  is the growth position, and the QW is centered at  $z=0$ . The diffusion coefficients are obtained by fitting the diffusion model to the measured concentration data [6] by using least square to minimize the error. Then, by discretizing the diffusion equations into time and position steps, and by using the as-grown profile as the initial condition, the partial differential equations are solved. The solution to the finite difference method gives rise to the concentrations of the diffused species as a profile across the system normalized over the system. The concentration of Al,  $C_3$ , is obtained by  $C_3 = 1 - C_1 - C_2$  which is the stoichiometry boundary condition.

The compositional profiles in the DFQW structure imply that the carrier effective mass, the bulk band gap, the strain and its effects vary continuously across the QW if the well is within the critical thickness regime. Subsequently the carrier effective mass  $m_r^*(z)$  will  $z$ -dependent and it is in the form  $m_r^*(z) = m_r^*(C_1, C_2)$ , where  $m_r^*(x, y)$  is the respective carrier  $\text{In}_x\text{Ga}_y\text{Al}_{1-x-y}\text{As}$  bulk effective mass, and  $r$  denotes either the electron C, heavy hole ( $V=HH$ ) or light hole ( $V=LH$ ). The unstrained (bulk) band gap in the well,  $E_g(C_1, C_2)$ , is also a function of the compositional profiles, so that the unstrained potential profile after interdiffusion,  $\Delta E_r(C_1, C_2)$ , varies across the well and is given by

$$\Delta E_r(C_1, C_2) = Q_r \Delta E_g(C_1, C_2), \quad (4)$$

where  $Q_r$  is the band offset and  $\Delta E_g$  is the unstrained bandgap offset.

## B. Effects of strain

The in-plane strain,  $\epsilon(C_1, C_2)$ , across the well will vary so that the strain effects are also  $z$ -dependent. Assuming that the growth direction  $z$  is along  $\langle 001 \rangle$ , then for the biaxial stress parallel to the interface the strain components, after interdiffusion, are given by[7]:

$$\begin{aligned} \epsilon_{xx} &= \epsilon_{yy} = \epsilon(C_1, C_2) \\ \epsilon_{zz} &= -2[c_{12}(C_1, C_2)/c_{11}(C_1, C_2)]\epsilon(C_1, C_2) \\ \epsilon_{xy} &= \epsilon_{yz} = \epsilon_{zx} = 0 \end{aligned} \quad (5)$$

where  $\epsilon(C_1, C_2)$  is misfit factor between the well and the barrier and is defined to be negative for compressive strain, and  $c_{ij}(C_1, C_2)$  are the elastic stiffness constants. The change in the bulk bandgap,  $S_{\perp}(C_1, C_2)$ , due to the biaxial component of strain is given by[7]:

$$S_{\perp}(C_1, C_2) = -2a(C_1, C_2)[1 - c_{12}(C_1, C_2)/c_{11}(C_1, C_2)]\epsilon(C_1, C_2) \quad (6)$$

where  $a(C_1, C_2)$  is the hydrostatic deformation potential calculated from[7]:

$$a(C_1, C_2) = -\frac{1}{3}[c_{11}(C_1, C_2) + 2c_{12}(C_1, C_2)]\frac{dE_g(C_1, C_2)}{dP} \quad (7)$$

where  $dE_g/dP$  is the hydrostatic pressure coefficient of the lowest direct energy gap  $E_g$ . The splitting energy,  $S_{//}(C_1, C_2)$ , between the HH and LH band edges induced by the uniaxial component of strain is given by[7]:

$$S_{//}(C_1, C_2) = -b(C_1, C_2)[1 + 2c_{12}(C_1, C_2)/c_{11}(C_1, C_2)]\epsilon(C_1, C_2) \quad (8)$$

where  $b(C_1, C_2)$  is the shear deformation potential. The parameters  $a$ ,  $b$ ,  $c_{ij}$ ,  $dE_g/dP$  in above equations are assumed to obey Vegard's law[8], so that their respective values depend directly on the compositional profiles across the QW. In the case of InGaAs/GaAs it is assumed that the LH and spin-orbit band are coupled due to the presence of the stress while the HH state remains uncoupled. The valence band splitting at  $\Gamma$  for the HH band and for the LH band are given by:

$$S_{//HH}(C_1, C_2) = S_{//}(C_1, C_2) \quad (9)$$

$$S_{//LH}(C_1, C_2) = 1/2[S_{//}(C_1, C_2) + \Delta_0(C_1, C_2)] + 1/2[9\{S_{//}(C_1, C_2)\}^2 + \{\Delta_0(C_1, C_2)\}^2 - 2S_{//}(C_1, C_2)\Delta_0(C_1, C_2)]^{1/2} \quad (10)$$

respectively, where  $\Delta_0(C_1, C_2)$  is the spin-orbit splitting. The QW confinement potential after the disordering process,  $U_r(C_1, C_2)$ , is obtained by modifying the unstrained potential profile after processing,  $\Delta E_r(C_{In}, C_{Al})$ , by the variable strain effects, and is given by:

$$U_r(C_1, C_2) = \Delta E_r(C_1, C_2) - S_{\perp r}(C_1, C_2) \pm S_{//r}(C_1, C_2) \quad (11)$$

where  $S_{\perp r}(C_1, C_2) = Q_r S_{\perp}(C_1, C_2)$ , the '+' and '-' signs represent the confined HH and LH profiles, respectively, and  $S_{//r}(C_1, C_2) = 0$ .

### C. Sub-band-edge calculation

To calculate the electron and hole wave function in QW, we use the multiband effective mass theory. A parabolic bands model and Luttinger-Kohn- Hamiltonian with strain components are used for the conduction and valence bands respectively. The electron states near the conduction subband edge are assumed to be almost purely s-like and nondegenerate (excluding spin), while the hole states near the valence subband edge are almost purely p-like and four-fold degenerate (including spin). The envelope function scheme is adopted to describe the slowly varying (spatially extended) part of the wavefunction.

The wavefunctions of the electron and hole subband edge at the zone centre of  $\Gamma$  valley symmetry can be calculated separately, using the Ben-Daniel and Duke model by the one-dimensional Schrodinger-like equation, which is written as follows:

$$-\frac{\hbar^2}{2} \frac{d}{dz} \left[ \frac{1}{m_r^*(z)} \frac{d\Psi_{rl}(z)}{dz} \right] + U_r(z) \cdot \Psi_{rl}(z) = E_{rl} \Psi_{rl}(z) \quad (12)$$

where  $\Psi_{rl}(z)$  is the wavefunction of the  $l^{\text{th}}$  subband for electrons ( $r=cl$ ) or holes ( $r=vl$ ), respectively;  $m_r^*(z)$  is the corresponding carrier effective mass in the  $z$  direction;  $E_{rl}$  is the subband-edge energy. Equation (12) is solved numerically using a finite difference method with the above confinement profile.

### 3. Results and Discussion

Table 1 shows the fitted interdiffusion coefficients which gave a rather surprising results in that the In-Ga diffusion coefficient is negative which means that the gradient of Ga will cause the inverse process of diffusion in In. Figure 1(a) shows Group III alloy concentration profile of as-grown  $\text{In}_{0.53}\text{Ga}_{0.47}\text{As}/\text{In}_{0.52}\text{Al}_{0.48}\text{As}$  DFQW with  $100\text{\AA}$  well width and  $250\text{\AA}$  thickness barrier. The In and Al as-grown content are set under lattice matched condition. Figure 1(b) and Figure 1(c) show the concentration profiles of the system with diffusion time of 1 hour and 3 hours at a temperature of  $812^\circ\text{C}$  respectively. It can be seen that both Al and Ga show smooth interdiffusion profiles. However, the In profile in Figure 1(b) shows a bouncing behavior at the interfaces. This is due to the fact that an inverse process of diffusion has been developed in In at the interfaces. At long diffusion time, all three species become smoothly distributed and the profiles are being lifted up at the well center implying all species have been diffused throughout the entire QW structure.

The confinement profiles show a double-welled structure in the well lager and a double barrier structure very similar to a resonant tunnel structure. This is because a consequence due to the frustration of In profiles. Eigen states exist both in the double-welled bottom potential and in the upper well top region. Well-to-well coupling does occur for the low energy states and tunneling enhancement also apply to the top most states. The transition energy C1-HH1 is shown in figure 3. A slow rate of increase of the bandgap occurs before 1 hour diffusion time and becomes quite rapidly after 3 hours.

The diffusion process can be used to tune the wavelength of InGaAs/InAlAs QW material in the region of  $1.5\mu\text{m}$  which is the optimum wavelength for operation of fiber optic systems with the lowest attenuation. In addition to shifting the operating wavelength, the effect of tensile strain QW on the laser application which is the first light-hole subband as the top valence subband can perform a smaller threshold current density as well as compressive strained QW. Moreover, this material system can also be used to develop both electro-absorptive and electro-refractive modulators in the optimum wavelength so that an integration of these optoelectronic devices can be developed in next stepped.

Table 1 The experimental data fitted interdiffusion coefficients of $\text{In}_{0.53}\text{Ga}_{0.47}\text{As}/\text{In}_{0.52}\text{Al}_{0.48}\text{As}$				
	In-In	In-Ga	Ga-In	Ga-Ga
$D_{ij}$	2.98	-4.01	0.18	6.69
Unit:	$10^{-18} \text{ cm}^2 \cdot \text{s}^{-1}$			

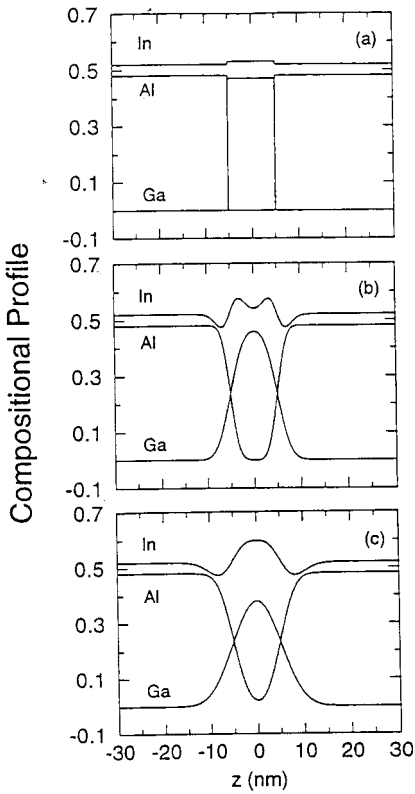


Figure 1. Compositional Profiles of  $\text{In}_{0.53}\text{Ga}_{0.47}\text{As}/\text{In}_{0.52}\text{Al}_{0.48}\text{As}$  with well width 100Å at 812 °C. (a) As-grown; (b) diffused for 1 hour; (c) diffused for 3 hours.

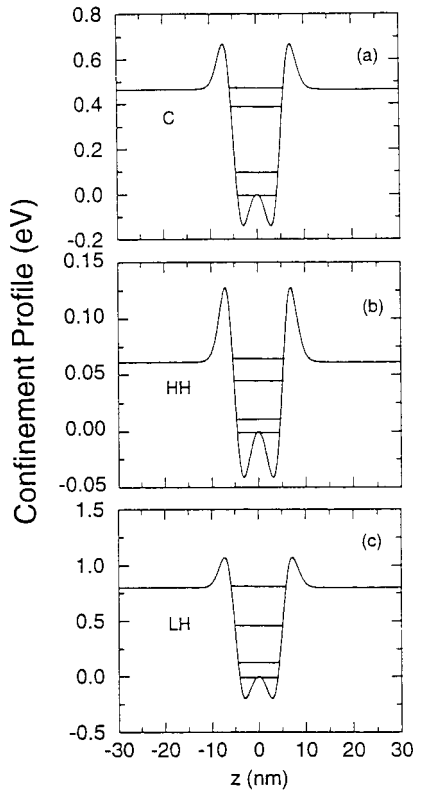


Figure 2. The Confinement profiles, and confined subband states for (a) electron, (b) HH, (c) LH of  $\text{In}_{0.53}\text{Ga}_{0.47}\text{As}/\text{In}_{0.52}\text{Al}_{0.48}\text{As}$  interdiffusion for 1 hour.

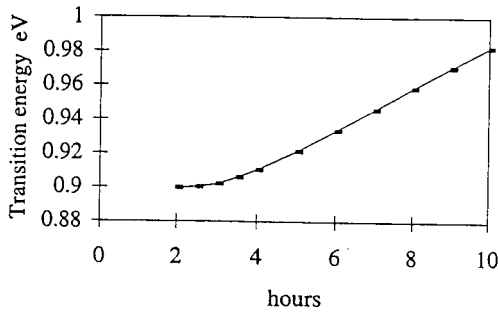


Figure 3. The transition energy Cl-HH1 of  $\text{In}_{0.53}\text{Ga}_{0.47}\text{As}/\text{In}_{0.52}\text{Al}_{0.48}\text{As}$ .

#### 4. Conclusions

In this work, the three species cations interdiffusion has been modeled base on the expanded Fick's second law. Results were fitted with experimental data and individual diffusion coefficients were determined. It is found that the Ga-Ga diffusion coefficient is relatively large in comparison to the other rates so that the Ga concentration profiles show some broadening on annealing. It is also found that the In-Ga diffusion coefficient is negative which gives rise to the inverse process of diffusion, causes sudden abrupt change in In profiles at the interfaces. All this would have important consequence in the understanding of the interdiffusion mechanism in multiple species of multiple alloy QW materials.

#### 5. Acknowledgment

The authors acknowledge the financial support of the RGC Research Grants and the HKU-CRGC Research Grants.

#### 6. References

- [1] K. Y. Cheng, A. Y. Cho, T. J. Drummound, and H. Morkoc, *Appl. Phys. Lett.* **40**, 147 (1982).
- [2] A. Kastalasky, R. Dingle, K. Y. Cheng, and A. Y. Cho, *Appl. Phys. Lett.* **41**, 274 (1982).
- [3] H. Temkin, K. Alavi, W. R. Wagner, T. P. Pearsall, and A. Y. Cho, *Appl. Phys. Lett.* **42**, 845 (1983).
- [4] D. F. Welch, D. W. Wicks, and L. F. Eastman, *Appl. Phys. Lett.* **43**, 762 (1983).
- [5] K. S. Seo, P. K. Bhattacharya, G. P. Kothiyal, and S. Hong, *Appl Phys. Lett.* **49** 966(1986).
- [6] R. J. Baird, T.J. Potter, G.P. Kothiyal, P.K. Bhattacharya, *Appl. Phys. Lett.* **52** 2055(1988).
- [7] H. Asai and K. Oe, *J. Appl. Phys.* **54** 2052 (1983).
- [8] R. People, *Phys. Rev. B.* **32** 1405 (1985).